

## *Analysis of Three-Phase Thyristor Phase Control Circuit with Series RLC Elements*

Toyoji HIMEI\*, Sen-ichiro NAKANISHI\*, Shigeyuki FUNABIKI\*,  
Hitoshi KOMATSUBARA\* and Osamu KUROSE\*\*

(Received November 24, 1982)

### Synopsis

An ac phase control circuit by thyristor is widely used in industry. The characteristics of the single-phase circuit with series *RLC* elements are numerically analyzed, and is reported the interesting phenomenon of step-up voltage without transformer. However, the performance of three-phase phase control circuit with series *RLC* elements is not made clear.

In this paper, the performance of three-phase control circuit of a balanced and an unbalanced load with series *RLC* elements is described. The analytical programs with each load are developed, and it is clarified that the calculated by this analytical program agree well with the measured. The calculated results, e.g. waveforms, RMS values of voltage and current, power, and power factor are illustrated and discussed the step-up phenomenon in three phase.

### 1. Introduction

An ac phase control circuit with an inverse parallel thyristor is widely used in industry, e.g. dimming, heat control, and speed control of motors, etc.<sup>1)</sup>. Then, the characteristics of the circuit are

---

\* Department of Electrical Engineering.

\*\* Graduate School of Electrical Engineering. Now, Mitsubishi Electric Co., Fukuyama Works.

numerically analyzed <sup>2-6)</sup>. Especially, it is reported that the single-phase phase control circuit with series *RLC* elements has the interesting phenomenon <sup>7,8)</sup>, that is a step-up phenomenon, and the phenomenon are also theoretically explained <sup>9)</sup>. However, the performance of three-phase phase control circuit with series *RLC* elements is not made clear.

In this paper, the performance of three-phase phase control circuit with series *RLC* elements <sup>10)</sup> is described. The operation of circuit is complicated due to a sequence of transient performances. At first, the circuit with delta balanced load is considered and investigated. Then, the waveforms and the step-up phenomenon are analyzed experimentally and theoretically. Namely, the transition of modes is decided from experimental waveforms and the state equations are derived. Then, the numerical analysis is in practice by using computer. Secondly, the performance of the circuit with delta unbalanced load is also carried out in the same way. Especially, the condition of transition of modes is clarified. Then, the analytical program is developed by using state equations. Besides, the behavior of power is illustrated in three dimensional display <sup>11)</sup> from the experimental results. The step-up phenomenon in this circuit are discussed as well as the balanced load.

## 2. Delta Balanced Load

### 2.1 Circuit and operating modes

A three-phase thyristor phase control circuit with series *RLC* elements is shown in Fig.1. The load is balanced in three phase.

The diagram of experimental circuit is illustrated in Fig.2. The relation between a source voltage and a phase control angle  $\alpha$  is shown in Fig.3. The square pulse with 150 degrees width is employed for a thyristor gate signal and the origin of time is set to a cross point of source voltage. Thyristors  $Th_1$ ,  $Th_6$ ,  $Th_3$ ,  $Th_2$ ,  $Th_5$ , and  $Th_4$  are fired in turn with 60 degrees

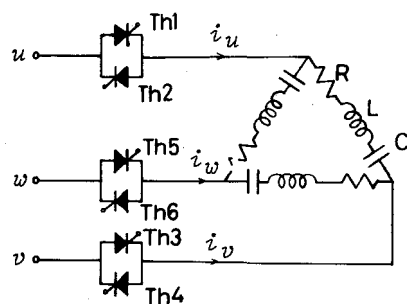


Fig.1 Three-phase thyristor phase control circuit with series *RLC* elements.

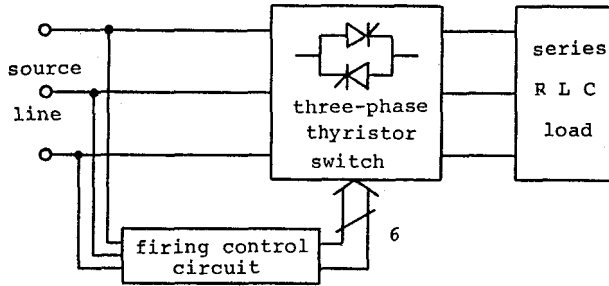


Fig.2 Diagram of experiment circuit.

interval.

In order to represent the characteristics of circuit in general, a displacement angle  $\phi$  of load between voltage and current and a damping factor  $\delta$  are employed as parameters. The parameters are defined as follows:

$$\phi = \tan^{-1} \left( \omega L - \frac{1}{\omega C} \right) / R, \quad (1)$$

$$\delta = \frac{R}{2} \sqrt{\frac{C}{L}}. \quad (2)$$

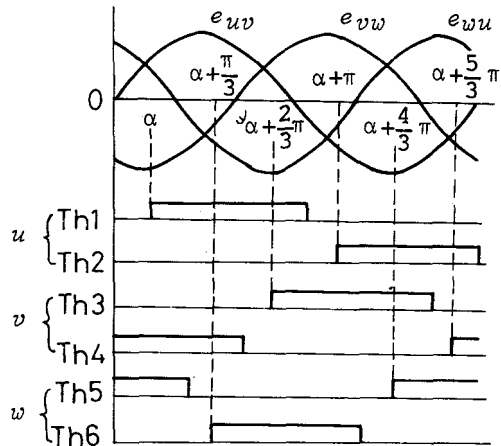
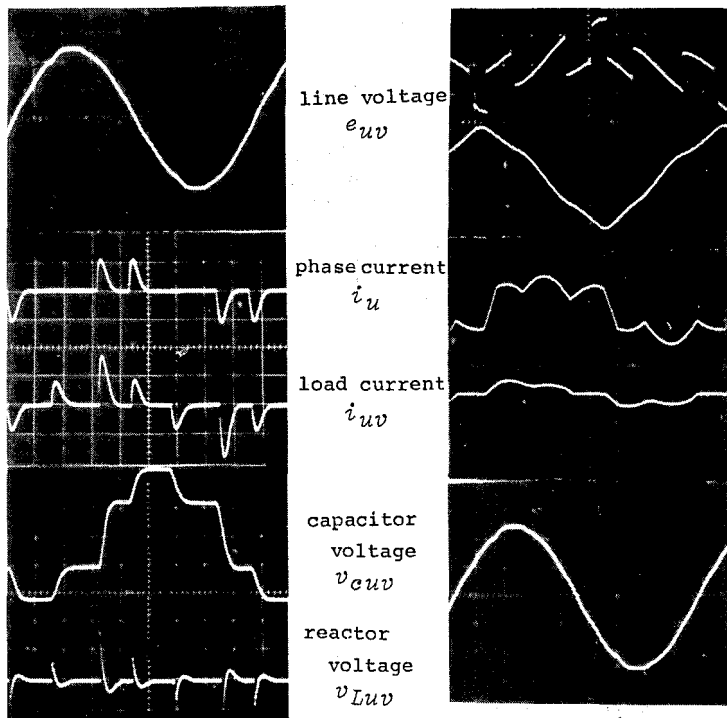


Fig.3 Sequence of thyristor gate pulses.

There are two cases of load current waveform corresponding to phase control angle  $\alpha$ . One of them is that the load current is discontinuous as shown in Fig.4(a). The other is the case in which the load current is continuous as shown in Fig.4(b). A capacitor voltage is charged in three steps as shown in this figure (a), and the load current has three pulse waveform in a half cycle. Thus, the state, in which the thyristor conduction angle is less than 60 degrees so that the current is discontinuous, is termed "State of Discontinuous Current" (mode I). While, the capacitor voltage is continuously charged and the load current changes in six steps in a half cycle in this figure (b), then the thyristor conduction angle is over 60 degrees so that



(a) state of discontinuous current (b) state of continuous current

Fig.4 Voltage and current waveforms in state of discontinuous and continuous current.

the load current is continuous. This state is termed "State of Continuous Current" (mode II).

Table 1 Boundary phase control angle  $\alpha_x$

$\phi$ (deg)	$\delta$	$\alpha_x$ (deg)
-76	0.5	50
-80	0.5	42
-80	0.58	36
-88	0.032	100

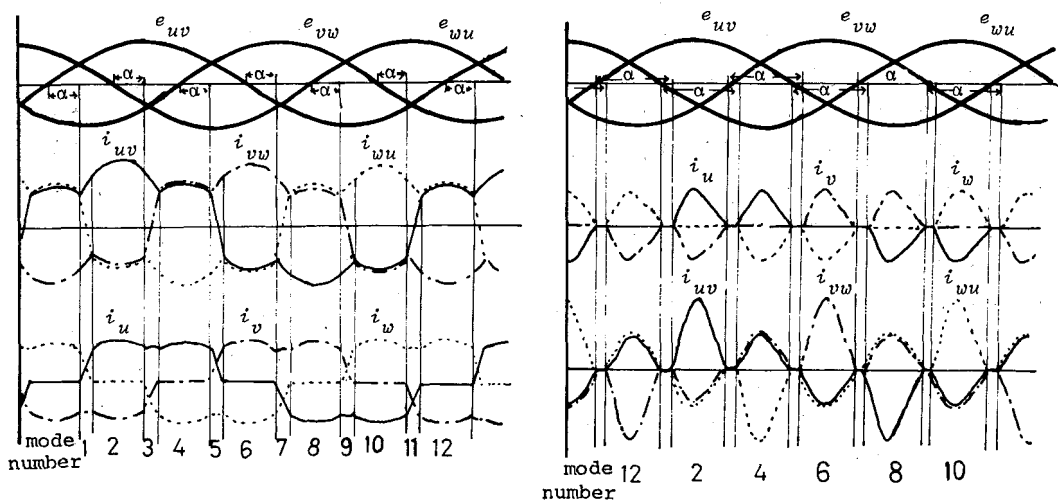
Generally, the alternative state mentioned above occurs in this circuit with delta connected load. The discontinuous state appears until the phase control angle  $\alpha_x$  and then the continuous state appears behind  $\alpha_x$ . The boundary phase control angles  $\alpha_x$  are shown in table 1.

The line voltages, the phase currents, and the load currents in

state of discontinuous current and continuous current are illustrated in Fig.5(a) and (b), respectively.

In state of continuous current (Fig.5(a)), each current is balanced with 120 degrees displacement due to a three-phase balanced load. Thus, the three-phase state and single-phase state appear alternatively, and also the each state appears every 60 degrees. Therefore, there are twelve modes which change in turn according to the number of mode shown in Fig.5(a). As shown in Fig.5(a) and Fig.6, mode 1 is a three-phase state where phase currents  $i_u$ ,  $i_v$ , and  $i_w$  flow, and then  $i_u$  increases and  $i_w$  decreases to zero. As soon as  $Th_5$  extinguishes, the single-phase state, mode 2, begins. In this mode,  $i_{vw}$  is equal to  $i_{wu}$ , and  $i_{uv}$  is duplicated. When  $Th_6$  is fired, the three-phase state, mode 3, begins. By this way, a similar change of mode is repeated. Though the source voltage  $e_{vw}$  reduces to zero in case of an inductive load,  $i_w$  doesn't become to zero.  $Th_5$  extinguishes after the polarity of  $e_{vw}$  changes and then  $i_w$  reduces to zero. If  $Th_6$  is fired at that time, it bursts into conduction because of the inverse polarity of  $e_{vw}$ , and mode 3 begins. Then, the odd number of mode in Fig.6 continues, or not, mode 2 begins.

As a phase control angle  $\alpha$  increases, a thyristor in other phase extinguishes before a thyristor in one phase bursts into conduction.



(a) state of continuous current (b) state of discontinuous current

Fig.5 Modes in state of continuous and discontinuous current.

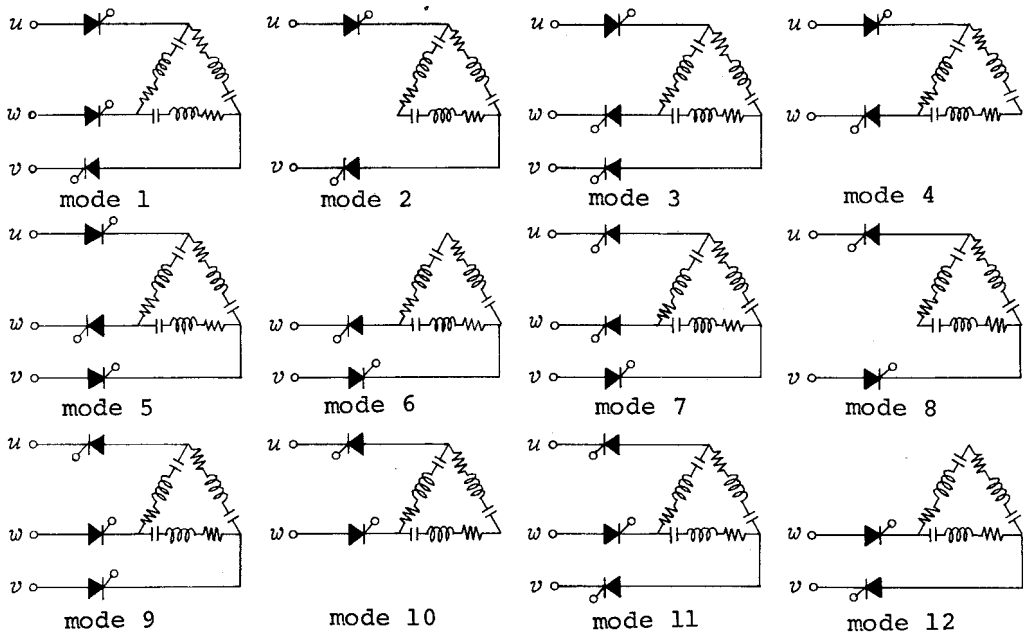


Fig.6 Operating modes in state of continuous current.

Therefore, the three-phase state doesn't exist and a state of discontinuous current, which repeats the single-phase mode, begins. For example, when  $Th_4$  and  $Th_1$  extinguish before  $Th_6$  is fired in mode 2, OFF state, in which all thyristors are open, begins. As soon as  $Th_1$  and  $Th_6$  are fired after then, a single-phase state begins again. Then, the even number of mode shown in Fig.6 continues. In case of the delta connected and balanced load, a circulating current doesn't exist in OFF state. However, if we assume that there is a circulating current  $i_3$  as shown in Fig.7, thus gain eq.(3).

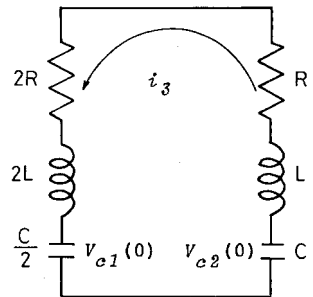


Fig.7 Circulating current in OFF state.

$$3Ri_3 + 3L \frac{di_3}{dt} = v_{c1} - v_{c2} \quad (3)$$

Now, the initial values of capacitor voltage  $v_{c1}$ ,  $v_{c2}$  are set to  $V_{c1}(0)$ , and  $V_{c2}(0)$ , so we get,

$$i_3 = \frac{V_{c1}(0) - V_{c2}(0)}{3R} \left(1 - e^{-\frac{L}{R}t}\right) \quad (4)$$

Therefore, a circulating current doesn't flow because  $V_{c1}(0)$  is equal to  $V_{c2}(0)$  in state of discontinuous current on account of a balanced load.

## 2.2 Numerical analysis

The numerical analysis in case of a delta connected and balanced load is carried out by means of the state variable analysis. In the analysis we introduce the following assumptions.

(1) The thyristor devices have the ideal characteristics. In other words, when the thyristor is closed, the forward voltage drop is zero. And when it is open, the forward leakage current is zero. Both turn off time and turn on time are equal to zero.

(2) All of the circuit constants are linear and the load is perfectly balanced.

(3) The waveform of supply voltage is sinusoidal and the source impedance is negligible.

(4) The thyristors are fired symmetrically every half cycle.

To begin with, we deal with the analysis of circuit performance in state of discontinuous current.

This circuit state is shown in Fig.8.

The differential equations of this circuit are expressed in matrix form. Herin, we set the instant time when the current begins to flow to the origin,

$$e_1 = \sqrt{2}E\sin(\omega t + \alpha),$$

$$e_2 = \sqrt{2}E\cos(\omega t + \alpha).$$

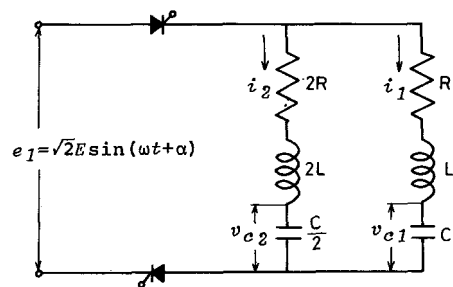


Fig.8 Circuit operation in state of discontinuous current.

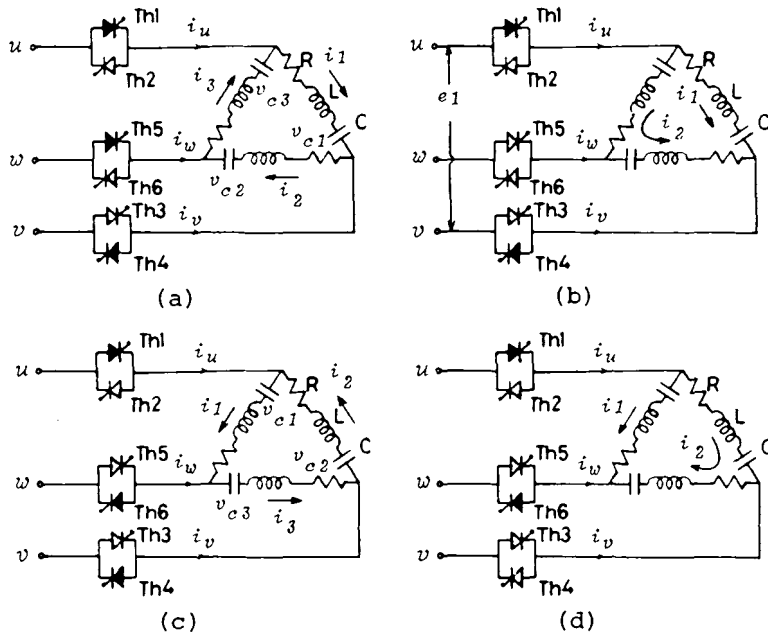


Fig.9 Examples of circuit operation in state of continuous current.

Then,

$$\mathbf{x}(t) = \begin{pmatrix} e_1 \\ e_2 \\ i_1 \\ i_2 \\ v_{c1} \\ v_{c2} \end{pmatrix} \quad (5) \quad \mathbf{A} = \begin{pmatrix} 0 & \omega & 0 & 0 & 0 & 0 \\ -\omega & 0 & 0 & 0 & 0 & 0 \\ 1/L & 0 & -R/L & 0 & -1/L & 0 \\ 1/2L & 0 & 0 & -R/L & 0 & -1/2L \\ 0 & 0 & 1/C & 0 & 0 & 0 \\ 0 & 0 & 0 & 2/C & 0 & 0 \end{pmatrix} \quad (6)$$



$v_{c2}$  is a sum of the capacitor voltages connected in series. However, this voltage must be separated as follows on changing mode,

$$\left\{ \begin{array}{l} v_{c21}(t) = \frac{v_{c2}(t) - (V_{c21}(0) + V_{c22}(0))}{2} + V_{c21}(0) \\ v_{c22}(t) = \frac{v_{c2}(t) - (V_{c21}(0) + V_{c22}(0))}{2} + V_{c22}(0) \end{array} \right. \quad (7)$$

Where,  $V_{c21}(0)$  and  $V_{c22}(0)$  are the final values in the last mode.

Secondly, we deal with the analysis in state of continuous current. There are two cases in three-phase state as shown in Fig.9(a) and (c) according to the direction of conducting thyristor. Where,  $e_{11}$  and  $e_{21}$  represent supply voltages,  $i_1, i_2, i_3$ ; load currents, and  $v_{c1}, v_{c2}, v_{c3}$ ; capacitor voltages.

$$\left\{ \begin{array}{l} e_{11} = i_1 R + L \frac{di_1}{dt} + v_{c1} \\ e_{21} = i_2 R + L \frac{di_2}{dt} + v_{c2} \\ -e_{21} - e_{11} = i_3 R + L \frac{di_3}{dt} + v_{c3} \\ \frac{dv_{c1}}{dt} = \frac{i_1}{C} \\ \frac{dv_{c2}}{dt} = \frac{i_2}{C} \\ \frac{dv_{c3}}{dt} = \frac{i_3}{C} \end{array} \right. \quad (8)$$

Where, we define the origin in time as well as in state of discontinuous current, and also

$$\begin{aligned}
 e_{11} &= \sqrt{2}E\sin(\omega t + \alpha) , \\
 e_{12} &= \sqrt{2}E\cos(\omega t + \alpha) , \\
 e_{21} &= \sqrt{2}E\sin(\omega t + \alpha - \frac{2}{3}\pi) , \\
 e_{22} &= \sqrt{2}E\cos(\omega t + \alpha - \frac{2}{3}\pi) .
 \end{aligned}$$

The state transition equations are expressed in matrix form as follows:

$$\alpha(t) = \begin{pmatrix} e_{11} \\ e_{12} \\ e_{21} \\ e_{22} \\ i_1 \\ i_2 \\ i_3 \\ v_{c1} \\ v_{c2} \\ v_{c3} \end{pmatrix} , \tag{9}$$

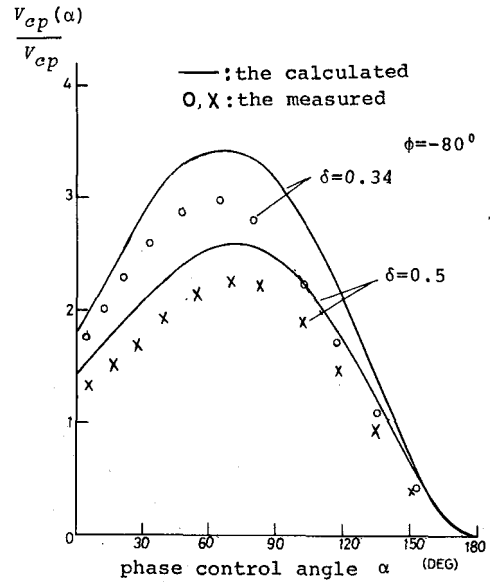


Fig.10 Comparison with the calculated and the measured.

$$A = \begin{pmatrix} 0 & \omega & 0 & 0 & 0 & 0 & 0 & 0 & 0 & 0 \\ -\omega & 0 & 0 & 0 & 0 & 0 & 0 & 0 & 0 & 0 \\ 0 & 0 & 0 & \omega & 0 & 0 & 0 & 0 & 0 & 0 \\ 0 & 0 & -\omega & 0 & 0 & 0 & 0 & 0 & 0 & 0 \\ 1/L & 0 & 0 & 0 & -R/L & 0 & 0 & -1/L & 0 & 0 \\ 0 & 0 & 1/L & 0 & 0 & -R/L & 0 & 0 & -1/L & 0 \\ -1/L & 0 & -1/L & 0 & 0 & 0 & -R/L & 0 & 0 & -1/L \\ 0 & 0 & 0 & 0 & 1/C & 0 & 0 & 0 & 0 & 0 \\ 0 & 0 & 0 & 0 & 0 & 1/C & 0 & 0 & 0 & 0 \\ 0 & 0 & 0 & 0 & 0 & 0 & 1/C & 0 & 0 & 0 \end{pmatrix} . \tag{10}$$

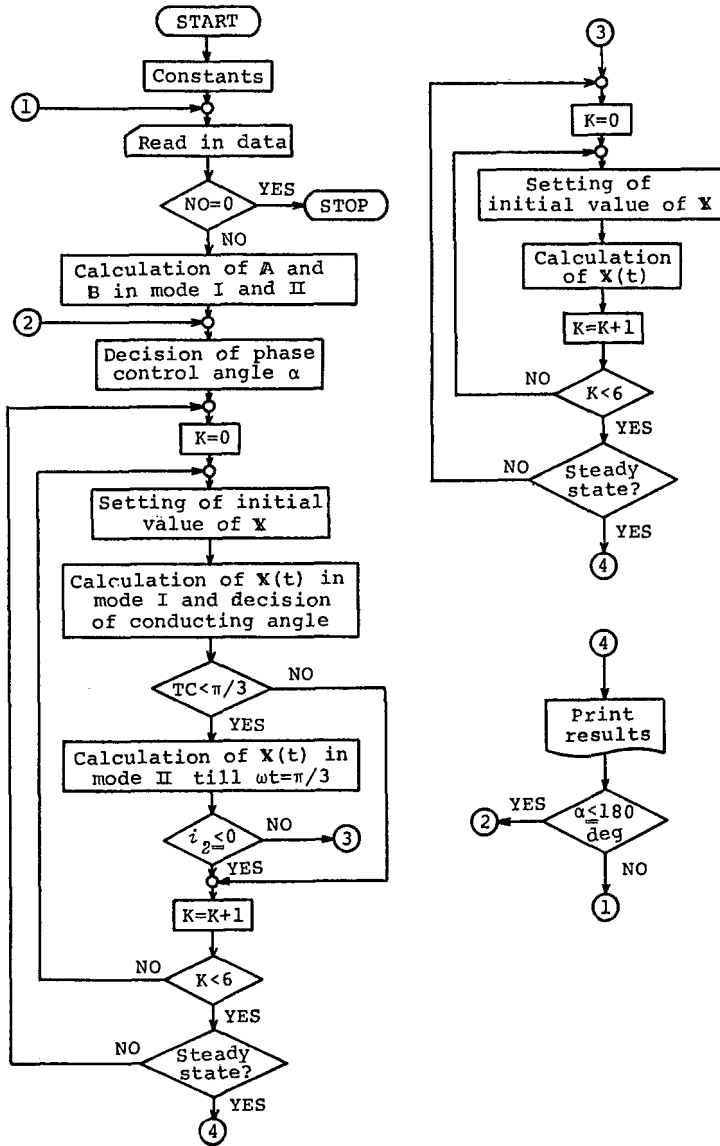


Fig.11 Flow chart of analytical program.

The comparison between the calculated and the measured is shown in Fig.10. There is a little deviation between them. The reasons of this deviation are as follows:

- (1) The load in three phase isn't perfectly balanced in experiment circuit .
- (2) The thyristors have a forward voltage drop.
- (3) The firing angles aren't perfectly symmetrical.
- (4) There are influences of the source impedance and its distorted waveform.

Fig.11 shows the flow chart of program for numerical analysis. A conduction angle in the operating mode in Fig.9(a) is calculated, at which  $i_2$  equals to  $i_3$ . If the resultant conduction angle is smaller than 60 degrees, the mode goes into the mode shown in Fig.9(b), or if larger, it goes into the mode shown in Fig.9(c). The operation in single-phase state is similar to that in state of discontinuous current.

2.3 Characteristics

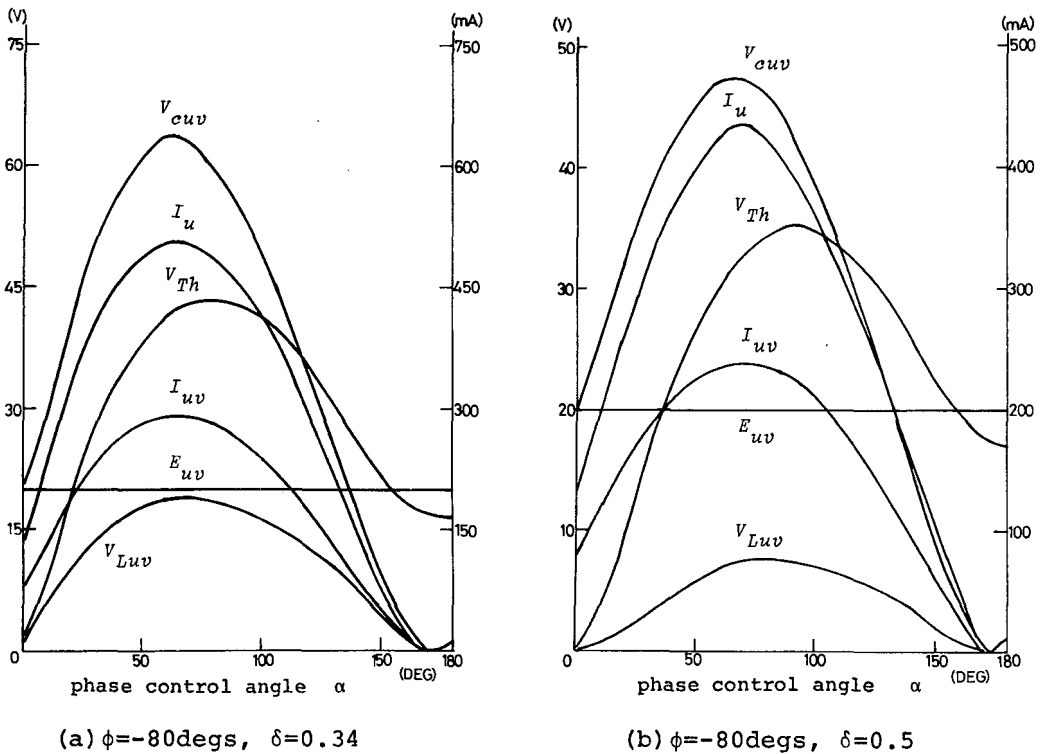


Fig.12 Step-up phenomenon.

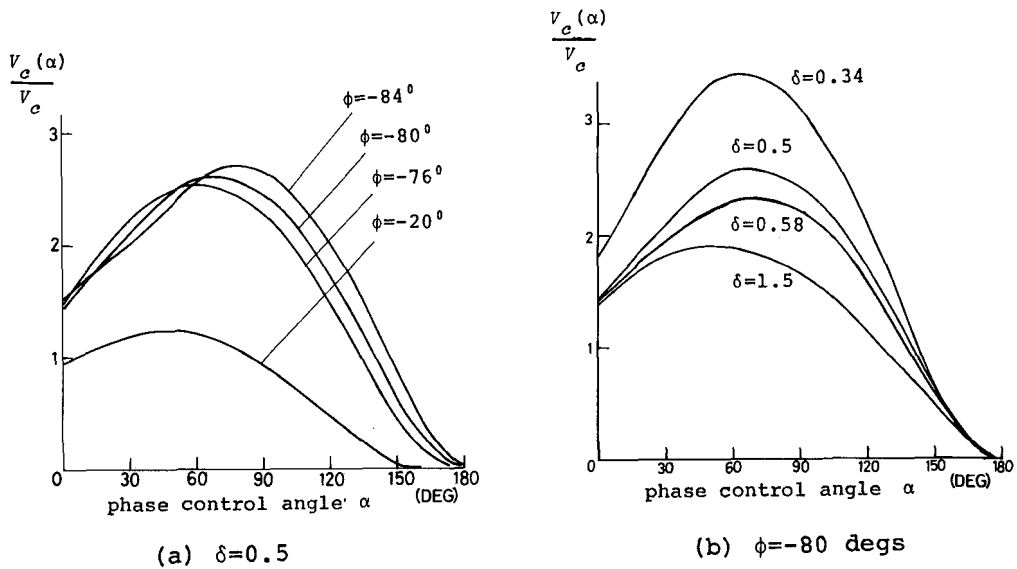


Fig.13 Step-up ratio of capacitor voltage.

Fig.12 shows the step-up phenomenon of thyristor voltage  $V_{Th}$ , capacitor voltage  $V_{cuv}$ , inductor voltage  $V_{Luv}$ , phase current  $I_u$ , and load current  $I_{uv}$ . Then, these values are normalized. The step-up ratio of capacitor voltage is shown in Fig.13 with parameters  $\phi$  and  $\delta$ . The step-up ratio is influenced by the load displacement angle  $\phi$ , the damping factor  $\delta$ , and the phase control angle  $\alpha$ . Especially, as  $\phi_2$  and  $\delta_2$  are smaller, the step-up ratio becomes larger.

The response time that the circuit performance becomes to be in steady state is numerically analyzed and the results are given in Table 2. As the maximum step-up ratio becomes larger, that is,  $\delta_2$  becomes smaller, the response time becomes longer. The phase control angle, at which the step-up ratio is maximum, also depends on  $\phi$ .

Table 2 Response time.

$\phi$ (deg)	$\delta$	$\alpha$ (deg)	response time
-76	0.5	60	5
-80	0.34	70	7
-80	0.5	70	5
-80	0.58	70	5
-80	0.83	70	5
-84	0.5	80	5
-88	0.22	90	11

### 3. Delta Unbalanced Load

#### 3.1 Circuit and experimental results

Fig.14 illustrates a three-phase circuit with delta unbalanced load. The experiment circuit and thyristor gate signals are the same as those with delta balanced load.

Fig.15 shows the capacitor voltage  $V_{c1}$ ,  $V_{c2}$ , and  $V_{c3}$  in experiment. The step-up phenomenon are observed as well as with delta balanced load. As the harmonics of current increase, the power factor decreases. Then, we investigate the behavior of harmonics as a cause of decreasing the power factor. The harmonics of phase current as shown in Fig.16 (a), (b), (c) increase as the phase control angle increases. Then, the contents of harmonics in current

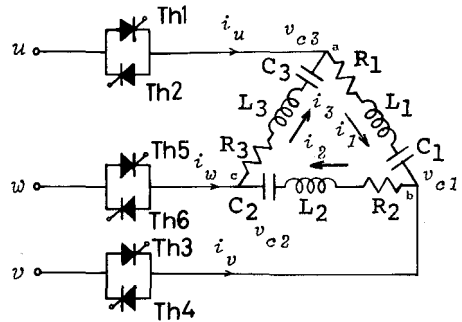


Fig.14 Three-phase thyristor phase control circuit with delta unbalanced load.

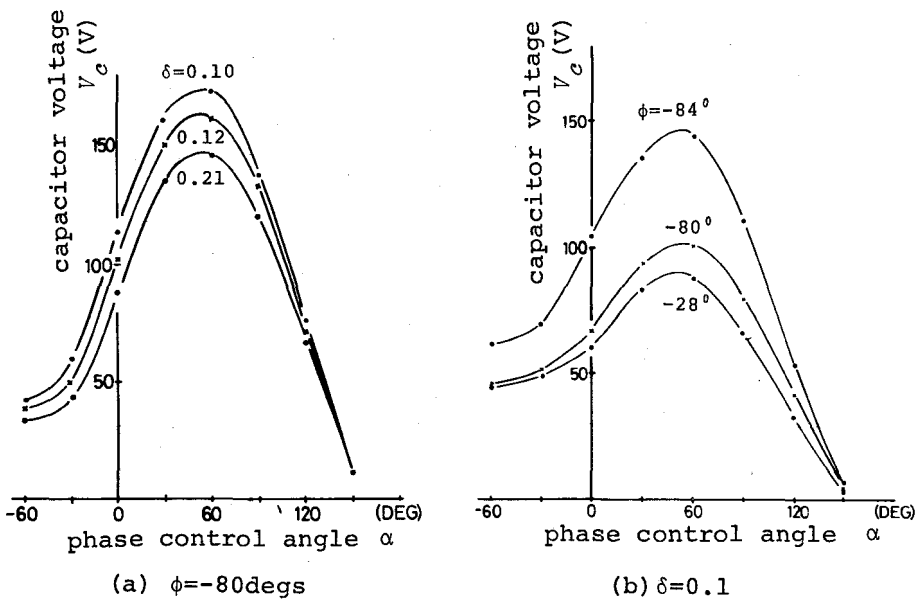


Fig.15 Characteristics of step-up phenomenon in capacitor voltage.

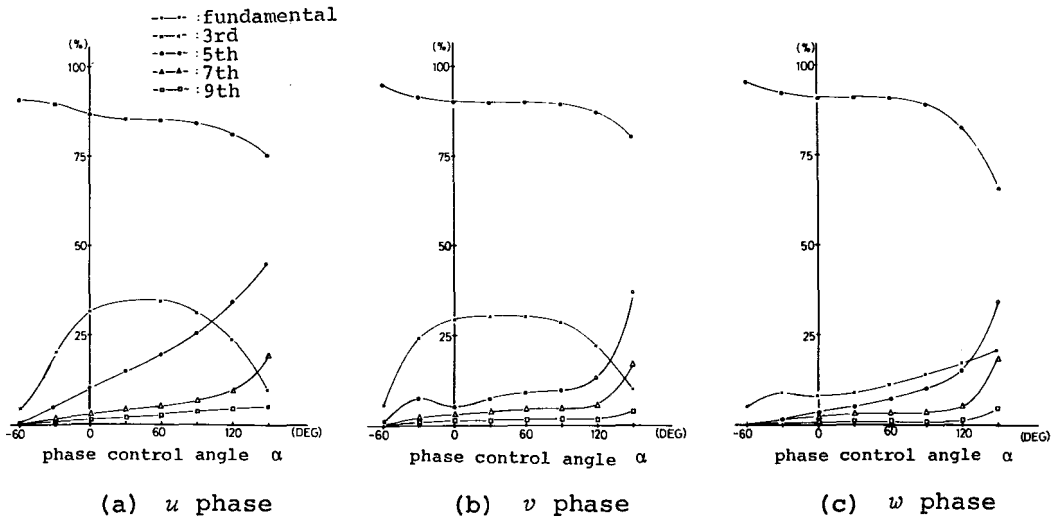


Fig.16 Harmonics analysis of current.

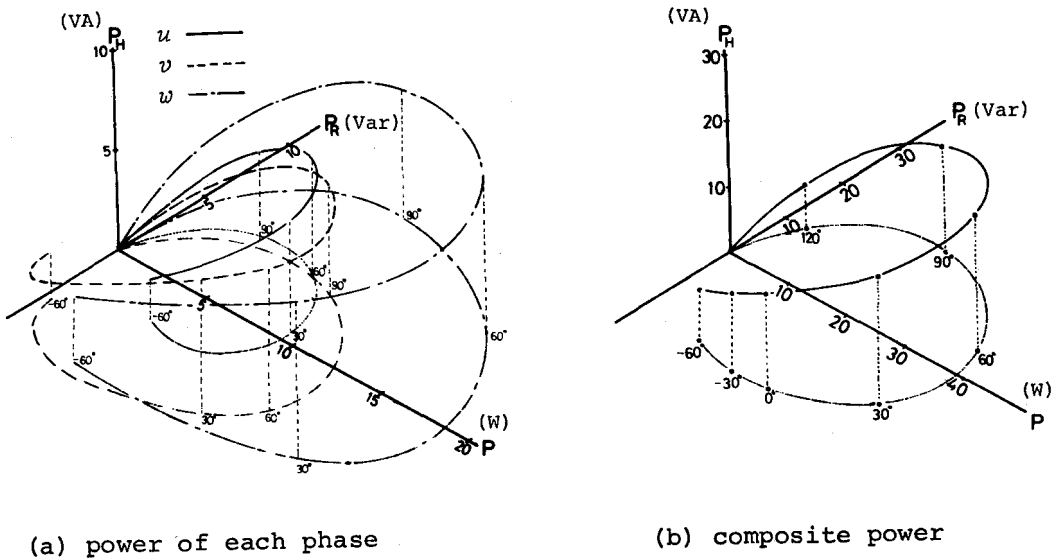


Fig.17 Three dimensional display of power.

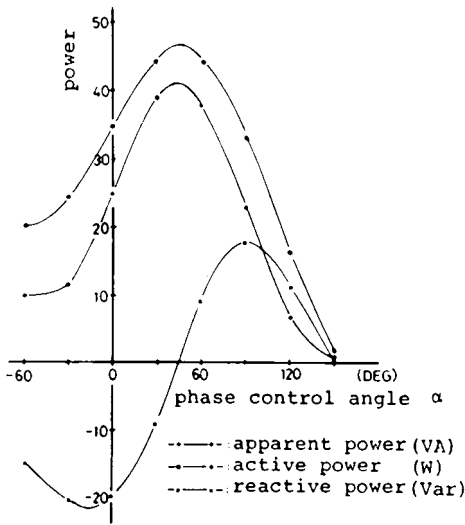


Fig.18 Control characteristics of power.

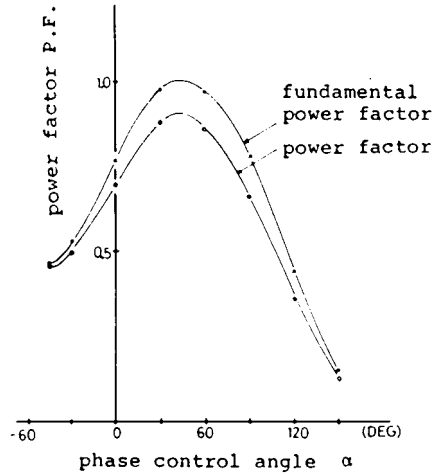


Fig.19 Power factor.

are about 70 percent at  $\alpha=150$  degrees. The distortion power  $P_H$  is got from this result. The apparent power  $P_A$  in each phase is expressed by phase current  $I$  and line voltage  $E$ .

$$P_A = E \cdot I / \sqrt{3} \tag{11}$$

The apparent power  $P_A$  is divided into active power  $P$ , reactive power  $P_R$ , and distortion power  $P_H$ .

$$P = E \cdot I \cdot k_1 \cdot \cos \phi_1 / \sqrt{3} \tag{12}$$

$$P_R = E \cdot I \cdot k_1 \cdot \sin \phi_1 / \sqrt{3} \tag{13}$$

$$P_H = E \sqrt{\sum_{n=3}^{\infty} I_n^2} / \sqrt{3} \tag{14}$$



Where,  $k_1$  is a ratio of fundamental component in phase current and  $\cos(\phi_1)$  is a fundamental power factor. The plot of  $P$ ,  $P_A$ , and  $P_H$  in a tridimension rectangular coordinate shown in Fig.17(a) shows the behavior of these powers. This figure (b) shows the tridimensional expression of composite power gained from the resultant vector in three phase. The control characteristics in power are shown in Fig.18.

Next, Fig.19 shows the variation of powr factor and fundamental power factor, which are varied with phase contorl angle  $\alpha$ . There are little harmonics component on non-control so that the power factor nearly equal to fundamental power factor on non-control. Then, the power factor is maximum when the reactive power  $P_R$  doesn't exist.

The step-up ratio, the RMS value of phase current, the active power, and the distortion power are maximum at the control angle  $\alpha$  at which the power factor is maximum. The reactive power  $P_R$  is zero at this angle as shown in Fig.17.

### 3.2 Operating mode

There are three kinds of mode according to the phase control angle  $\alpha$ . These modes are shown in Fig.20. Three thyristors are closed in this figure (a) and the mode is termed "mode T". The figure (b) shows a single-phase state that two thyristors are closed and the mode is termed "mode S". Then, the thyristors in  $u$  and  $v$  phase are closed in mode S1. The thyristors in  $v$  and  $w$  phase are closed in mode S2. The thyristors in  $w$  and  $u$  phase are closed in mode S3. All of the thyristors of three phases are open in mode C.

Though the twelve modes change in turn in case of the balanced load

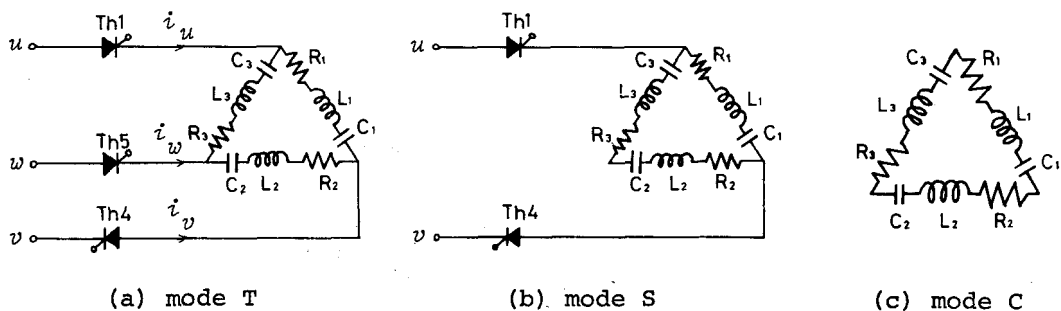


Fig.20 Three kinds of operating modes.

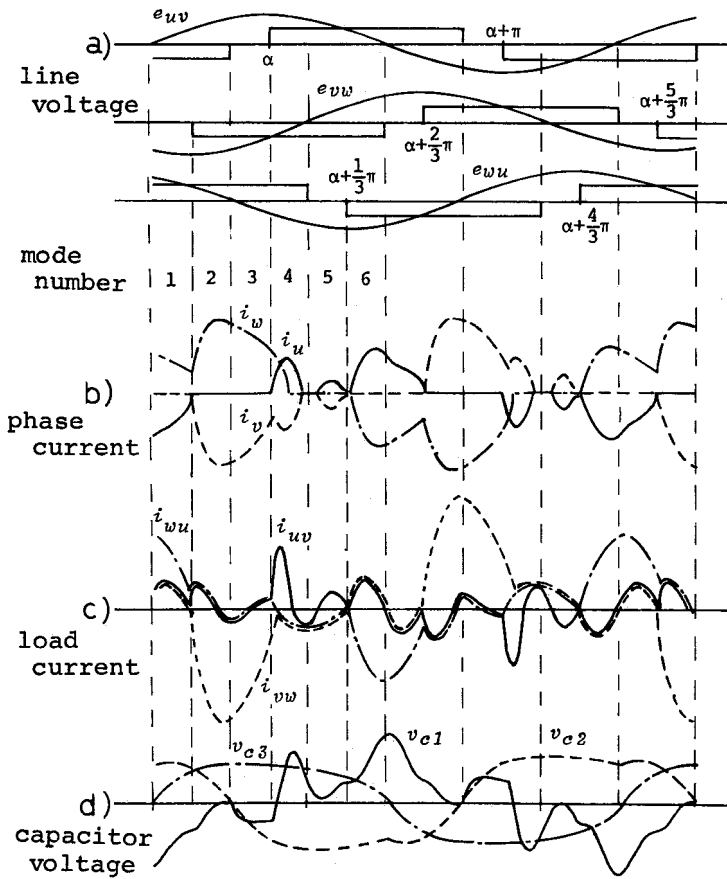


Fig.21 Voltage and current waveforms.

Table 3 Circuit constants.

$R_1$ ( $\Omega$ )	$L_1$ (mH)	$C_1$ ( $\mu F$ )	$R_2$ ( $\Omega$ )	$L_2$ (mH)
60	110	1	60	110
$C_2$ ( $\mu F$ )	$R_3$ ( $\Omega$ )	$L_3$ (mH)	$C_3$ ( $\mu F$ )	
10	60	110	10	

mentioned in section 2, the mode doesn't change in turn in the circuit with the unbalanced load. When we investigate the characteristics with the balanced load, it is sufficient to take note of only one phase. However, we must take note of all of the performance in three phase in the circuit with the unbalanced load. Setting the currents flowing through thyristors  $Th_1-Th_6$  to  $i_{Th1}-i_{Th6}$ , we gain the next relation.

$$\begin{bmatrix} i_{Th1} \\ i_{Th2} \\ i_{Th3} \\ i_{Th4} \\ i_{Th5} \\ i_{Th6} \end{bmatrix} = \begin{bmatrix} 1 & 0 & 0 \\ -1 & 0 & 0 \\ 0 & 1 & 0 \\ 0 & -1 & 0 \\ 0 & 0 & 1 \\ 0 & 0 & -1 \end{bmatrix} \begin{bmatrix} i_u \\ i_v \\ i_w \end{bmatrix} = \begin{bmatrix} 1 & 0 & -1 \\ -1 & 0 & 1 \\ 0 & -1 & 1 \\ 0 & 1 & -1 \\ -1 & 1 & 0 \\ 1 & -1 & 0 \end{bmatrix} \begin{bmatrix} i_1 \\ i_2 \\ i_3 \end{bmatrix} \quad (15)$$

The conditions of turn-on of thyristor are next two.

- 1) The thyristor is impressed by voltage in forward direction.
- 2) The thyristor is fired.

Besides, the condition of turn-off thyristor is that the currents  $i_{Th1}-i_{Th6}$  decrease to zero. The analysis in transition of mode is carried out by using both conditions. The relations among line voltage, phase current, load current, and capacitor voltage are shown in Fig.21.

The relations of line voltage and gate pulse in each phase are shown in the figure (a). The figure (b) shows the waveform of phase current  $i_u$ ,  $i_v$ , and  $i_w$ . The figure (c) shows the load current  $i_{uv}$ ,  $i_{vw}$ , and  $i_{wu}$ . The figure (d) shows the capacitor voltages  $v_{c1}$ ,  $v_{c2}$ , and  $v_{c3}$ . The phase control angle  $\alpha$  is 90 degrees in this figure. The change of mode is as follows from the waveforms of  $i_u$ ,  $i_v$ , and  $i_w$  in the figure (b). It is "mode S3" that two thyristors  $Th_2$  and  $Th_5$  are closed in state 1. It is "mode S2" that thyristor  $Th_2$  extinguishes and thyristor  $Th_4$  bursts into conduction, and two thyristor  $Th_4$  and  $Th_5$  are closed in state 2. In state 3, it is the same as in state 2. Thyristor  $Th_1$  bursts into conduction, and thyristor  $Th_1$ ,  $Th_4$ , and  $Th_5$  are closed in state 4 which is termed, "mode T". Then, thyristor  $Th_5$  extinguishes so that mode S1 begins. Thyristors  $Th_1$  and  $Th_4$  extinguish at the same time, then mode C begins. In this mode, the circulating current flows through the load. Next, as thyristors  $Th_1$  and  $Th_4$  burst into conduction

together, mode S1 begins. In state 6, thyristor  $Th_4$  extinguishes and thyristor  $Th_6$  bursts into conduction, and then mode S3 begins. After then, the mode change occurs.

The above-mentioned is an example of change of mode. However, there are many types of change according to the circuit constants. But, the conditions of turn-off of each thyristor are same. In fact, as shown in Fig.21(b), it is noted that the forward voltage of each thyristor isn't taken account of at all in mode T and mode S. Because each thyristor turns on at the same time that the gate pulse is impressed. As soon as the thyristor is expressed the forward voltage and fired in mode C shown in Fig.21(b), it bursts into conduction. Therefore, only when mode C changes to other mode, the forward voltage must be taken account of as a condition of turn on. It is also noted that a moment when the currents  $i_{Th1} - i_{Th6}$  decrease to zero must be taken account of as a condition of turn off.

### 3.3 Numerical analysis

As mentioned above, there are three kinds of mode; mode T, mode S, and mode C in the circuit performance. In order to analyze the performance of circuit, it is necessary to formulate the characteristic equations in each mode. In case of a delta balanced load, the equations are matrix forms. At first, the differential matrix equations are derived as follows;

(1) mode T

The circuit operation in mode T is shown in Fig.20(a). Observing between  $u$  phase and  $v$  phase, we obtain,

$$L_1 \frac{di_1}{dt} + R_1 i_1 + v_{c1} = e_{uv} = \sqrt{2}E \sin \omega t, \quad (16)$$

$$i_1 = C_1 \frac{dv_{c1}}{dt}. \quad (17)$$

Observing between  $v$  phase and  $w$  phase, we obtain,

$$L_2 \frac{di_2}{dt} + R_2 i_2 + v_{c2} = e_{vw} = \sqrt{2}E \sin(\omega t - \frac{2}{3}\pi), \quad (18)$$

$$i_2 = C_2 \frac{dv_{c2}}{dt} \quad (19)$$

Observing between  $w$  phase and  $u$  phase, we obtain,

$$L_3 \frac{di_3}{dt} + R_3 i_3 + v_{c3} = e_{wu} = \sqrt{2}E \sin(\omega t - \frac{4}{3}\pi) \quad (20)$$

$$i_3 = C_3 \frac{dv_{c3}}{dt} \quad (21)$$

(2) mode S

The circuit operation in mode S is shown in Fig.20(b). The characteristic equations are derived as follows in mode S1, S2, and S3, respectively.

(i) mode S1

Observing between  $u$  phase and  $v$  phase, we obtain,

$$L_1 \frac{di_1}{dt} + R_1 i_1 + v_{c1} = e_{uv} \quad (22)$$

$$i_1 = C_1 \frac{dv_{c1}}{dt} \quad (23)$$

From  $vw$  and  $wu$ , we obtain,

$$(L_2 + L_3) \frac{di}{dt} + (R_2 + R_3) i + v_c = -e_{uv} \quad (24)$$

$$i = \frac{C_2 C_3}{C_2 + C_3} \cdot \frac{dv_c}{dt} \quad (25)$$

where,  $i = i_2 = i_3$ ,  $v = v_{c2} + v_{c3}$ .

(ii) mode S2

From  $uv$  and  $wu$ , we obtain,

$$(L_3+L_1) \frac{di}{dt} + (R_3+R_1)i + v_c = -e_{vw} , \quad (26)$$

$$i = \frac{C_3 C_1}{C_3+C_1} \cdot \frac{dv_c}{dt} , \quad (27)$$

where,  $i=i_3=i_1$ ,  $v_c=v_{c3}+v_{c1}$ .Observing between  $v$  phase and  $w$  phase, we obtain,

$$L_2 \frac{di_2}{dt} + R_2 i_2 + v_{c2} = e_{vw} , \quad (28)$$

$$i_2 = C_2 \frac{dv_{c2}}{dt} . \quad (29)$$

(iii) mode S3

From  $uv$  and  $vw$ , we obtain,

$$(L_1+L_2) \frac{di}{dt} + (R_1+R_2)i + v_c = -e_{wu} , \quad (30)$$

$$i = \frac{C_1 C_2}{C_1+C_2} \cdot \frac{dv_c}{dt} , \quad (31)$$

where,  $i=i_1=i_2$ ,  $v_c=v_{c1}+v_{c2}$ .Observing between  $w$  phase and  $u$  phase, we obtain,

$$L_3 \frac{di_3}{dt} + R_3 i_3 + v_{c3} = e_{wu} , \quad (32)$$

$$i_3 = C_3 \frac{dv_{c3}}{dt} . \quad (33)$$

When the capacitor voltage  $v_c$  is separated, eq.(6) is used.

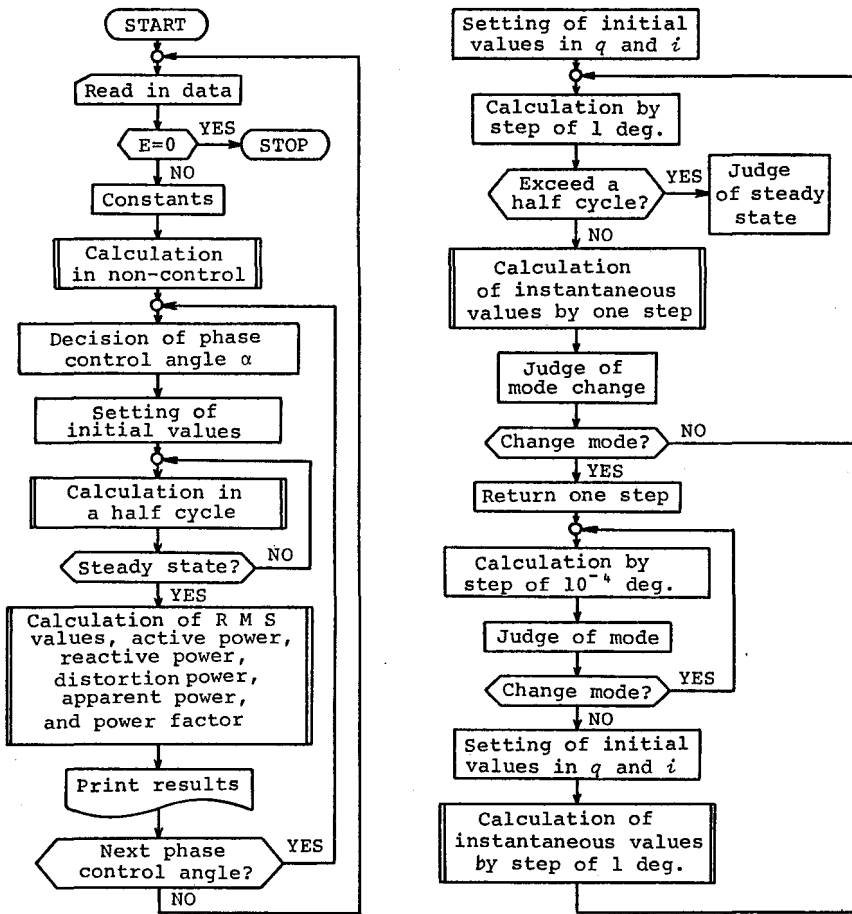
(3) mode C

The circuit in mode C is shown in Fig.20(c). The circuit equations is as follows:

$$(L_1+L_2+L_3) \frac{di}{dt} + (R_1+R_2+R_3)i + v_c = 0 \quad , \quad (34)$$

$$i = \frac{C_1 C_2 C_3}{C_1 C_2 + C_2 C_3 + C_3 C_1} \cdot \frac{dv_c}{dt} \quad . \quad (35)$$

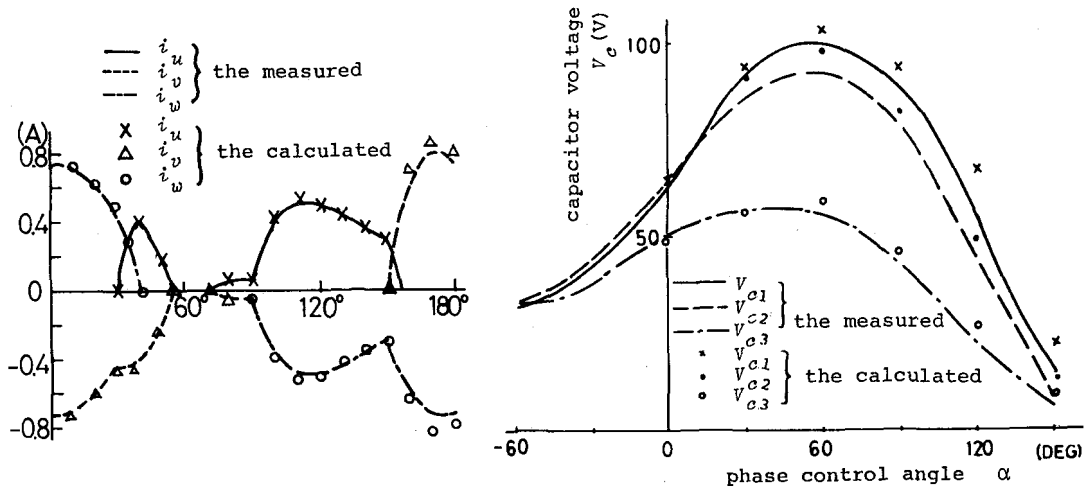
where,  $i=i_1=i_2=i_3$ , and  $v_c=v_{c1}+v_{c2}+v_{c3}$ .



(a) main program

(b) flow chart in a half cycle

Fig.22 Flow chart of computer program.



(a) instantaneous values (b) RMS values of capacitor voltage

Fig.23 Comparison with calculated and the measured.

The characteristic equations (16)-(35) can be solved, respectively. The capacitor voltages  $v_{c1}$ ,  $v_{c2}$ ,  $v_{c3}$ , the load currents  $i_1$ ,  $i_2$ ,  $i_3$ , and those differentiation  $di_1/dt$ ,  $di_2/dt$ ,  $di_3/dt$  are represented as a function of initial conditions, time  $t$ , and the displacement angle  $\phi$ . The origin of time is set to the starting point of every mode.

The flow chart of analytical program of the three-phase thyristor phase control circuit with unbalanced load is shown in Fig.22. Source voltage  $E$ , circuit constants  $R_1, R_2, R_3, L_1, L_2, L_3, C_1, C_2, C_3$ , phase control angle  $ALP$ , final phase control angle  $ALPL$  and increment of phase control angle  $DALP$  are available for input data. The calculation is carried out by step  $DALP$  from  $ALP$  to  $ALPL$ . Taking account of the turn on and turn off conditions, the final values of the capacitor voltages  $v_{c1}$ ,  $v_{c2}$ ,  $v_{c3}$  and the load currents  $i_1$ ,  $i_2$ ,  $i_3$  in  $uv, vw, wu$ , at the change of mode, are set to the initial values of next mode.

Then, the forward voltage of thyristor in OFF state is calculated in the following way. The forward voltage of  $Th_1-Th_6$  is represented as the differences of voltage between point  $u$  and  $a$ , point  $v$  and  $b$ , and point  $w$  and  $c$  shown in Fig.14. The thyristor impressed forward voltage isn't fired in the OFF state, then it can't burst into conduction so that this mode still continues. On account of the comparison with the calculated and the measured, the current waveform and effective value of capacitor are illustrated in Fig.23. A little deviation as compared



with them is found. The waveforms, however, are similar well. Consequently, the results of this analysis are considered to represent the correct performances of this circuit.

#### 4. Conclusions

The performance of the three-phase phase control circuit is described in experiment and numerical analysis. In the circuit with a delta balanced load, there are two states of circuit performance; "State of Continuous Current" and "State of Discontinuous Current". Then, three kinds of mode appear in turn which are three-phase state, single-phase state, and OFF state. The analytical program developed in this paper is found to be available from the comparison with the calculated and the measured. Secondly, as the transition of modes isn't in turn, in the circuit with a delta unbalanced load, a new analytical program is developed, and the transition of modes is automatically decided due to the thyristor switching. It is clarified in experiment and calculation that the step-up phenomenon appear in three-phase circuit as well as in the single-phase circuit, and the step-up phenomenon with the balanced load is different from those with the unbalanced load.

#### Acknowledgement

The authors would like to thank Mr. M. Sato, Mr. Y. Sato and Mr. K. Yamamoto, who were a research student and undergraduates in our chair, for their help in experiment and calculation at the first stage.

#### References

- 1) T. Hori: "Primary Voltage Control of Induction Motor Using Thyristor", Journal of The Japan Association of Automatic Control Engineers, Vol.11, No.6, p.314 (1967) (in Japanese)
- 2) W. Shepherd: "On the Analysis of the Three-Phase Induction Motor with Voltage Control by Thyristor Switching", IEEE Trans. Industr. Gen. Applic., Vol.IGA-4, No.3, p.304 (1968)

- 3) R.E. Bedford, Vilas D. Nene: "Voltage Control of the Three-Phase Induction Motor by Thyristor Switching: a Time-Domain Analysis the  $\alpha$ - $\beta$ -0 Transformation", IEEE Trans. Industr. Gen. Applic., Vol.IGA-6, No.6, p.553 (1970)
- 4) W. Shepherd: "Steady-State Analysis of Single-Phase Parallel Resistance-Inductance Circuits Controlled by SCR Pairs", IEEE Trans, Industr. Gen. Applic., Vol.IGA-1, No.4, p.259 (1965)
- 5) B.W. Lingard, R.W. Johnson, W. Shepherd: "Steady-State Performance and Analysis of the Series Resistance-Capacitance Circuit with Control by Adjustable Thyristor Triggering", IEEE Trans. Industr. Gen. Applic., Vol.IGA-4, No.6, p.644 (1968)
- 6) Eugene M. Perrin, Emil T. Schonhozer: "Fundamental Operation of Rectifiers with Thyristor AC Power Control", IEEE Trans. Industr. Applic., Vol.IA-9, No.4, p.453 (1973)
- 7) T. Himei, J. Inoue, S. Nakanishi: "Steady State Characteristics of Thyristor Control Circuit with a Series  $R$ - $L$ - $C$  Load", J.I.E.E., Vol.90, No.1, p.190, Jan. (1970) (in Japanese)
- 8) T. Himei, J. Inoue, S. Nakanishi, I. Ukita: "A Step-up Phenomenon of the Thyristor Control Circuit with Series  $RLC$  Elements", IEEE Trans., Industr. Applic., Vol.IA-11, No.5, p.531 (1975)
- 9) T. Himei, J. Inoue, S. Nakanishi: "Discussion on Series Resonance of Step-up Phenomenon in Thyristor Phase Control Circuit with  $RLC$  Elements", Paper of Technical Meeting on Transformers and Capacitors, TC-75-16 (1975) (in Japanese)
- 10) T. Himei, S. Nakanishi: "A Three Dimensional Expression of RMS Voltage and Current of the Phase Control Circuit by Thyristors having a Series Capacitor", J.I.E.E., Vol.96-B, No.7, p.333 (1976) (in Japanese)
- 11) T. Himei, S. Nakanishi: "A Step-up Phenomenon in the Three-Phase Thyristor Control Circuit", 1975-Chugoku Branch Joint Conv. Four Insts. Elec. Engrs. of Jap., No.20504 (in Japanese)